

Comprehensive Assessment of Myocardial Perfusion Defects, Regional Wall Motion, and Left Ventricular Function by Using 64-Section Multidetector CT¹

Ricardo C. Cury, MD
 Koen Nieman, MD
 Michael D. Shapiro, DO
 Javed Butler, MD
 Cesar H. Nomura, MD
 Maros Ferencik, MD, PhD
 Udo Hoffmann, MD
 Suhny Abbara, MD
 Davinder S. Jassal, MD
 Tsunehiro Yasuda, MD
 Herman K. Gold, MD
 Ik-Kyung Jang, MD
 Thomas J. Brady, MD

¹ From the Department of Radiology (R.C.C., K.N., M.D.S., J.B., C.H.N., M.F., U.H., S.A., T.J.B.), Cardiology Division (D.S.J., T.Y., H.K.G., I.J.), and Cardiac MR-PET-CT Program (R.C.C., K.N., M.D.S., J.B., C.H.N., M.F., U.H., S.A., T.J.B.), Massachusetts General Hospital and Harvard Medical School, 165 Cambridge St, Suite 400, Boston, MA 02114. From the 2006 RSNA Annual Meeting. Received August 19, 2007; revision requested October 8; revision received January 3, 2008; accepted February 4; final version accepted March 3. Supported in part by New York Cardiac Center, New York, NY, and Siemens Medical Solutions, Erlangen, Germany. M.F., M.D.S.; J.B. supported by NIH grant 1 T32 HL076136-02. K.N. supported by the Interuniversity Cardiology Institute of the Netherlands, Utrecht, the Netherlands. **Address correspondence to R.C.C.** (e-mail: rcury@partners.org).

© RSNA, 2008

Purpose:

To evaluate the accuracy of 64-section multidetector computed tomography (CT) for the assessment of perfusion defects (PDs), regional wall motion (RWM), and global left ventricular (LV) function.

Materials and Methods:

All myocardial infarction (MI) patients signed informed consent. The IRB approved the study and it was HIPAA-compliant. Cardiac multidetector CT was performed in 102 patients (34 with recent acute MI and 68 without). Multidetector CT images were analyzed for myocardial PD, RWM abnormalities, and LV function. Global LV function and RWM were compared with transthoracic echocardiography (TTE) by using multidetector CT. PD was detected by using multidetector CT and was correlated with cardiac biomarkers and single photon emission CT (SPECT) myocardial perfusion imaging. Multidetector CT diagnosis of acute MI was made on the basis of matching the presence of PD with RWM abnormalities compared with clinical evaluation.

Results:

Correlation between multidetector CT and TTE for global function ($r = 0.68$) and RWM ($\kappa = 0.79$) was good. The size of PD on multidetector CT had a moderate correlation against SPECT ($r = 0.48$, $-7\% \pm 9$). There was good to excellent correlation between cardiac biomarkers and the percentage infarct size by using multidetector CT ($r = 0.82$ for creatinine phosphokinase, $r = 0.76$ for creatinine phosphokinase of the muscle band, and $r = 0.75$ for troponin). For detection of acute MI in patients, multidetector CT sensitivity was 94% (32 of 34) and specificity was 97% (66 of 68). Multidetector CT had an excellent interobserver reliability for ejection fraction quantification ($r = 0.83$), as compared with TTE ($r = 0.68$).

Conclusion:

Patients with acute MI can be identified by using multidetector CT on the basis of RWM abnormalities and PD.

© RSNA, 2008

Supplemental material: <http://radiology.rsna.org/cgi/content/full/248/2/466/DC1>

The estimated incidence of ST segment elevation myocardial infarction (MI) is 400 000 patients per year in the United States alone (1). The risk of cardiac complications, such as recurrent acute MI, sudden death, angina pectoris, heart failure, and stroke for those who survive an acute MI is substantial (2). Appropriate risk stratification and management of patients with acute MI requires a comprehensive assessment of the coronary arteries (culprit vessel detection and overall coronary disease burden), global and regional left ventricular (LV) function, and infarct size. This information is vital for estimation of prognosis, as well as patient management. Currently, these data are acquired over several days of hospital admission, with the use of a variety of resources including echocardiography, single photon emission computed tomography (SPECT) myocardial perfusion imaging, cardiac magnetic resonance (MR) imaging, and invasive coronary angiography.

With advances in multidetector computed tomography (CT) technology, 64-section multidetector CT scanners

with submillimeter collimation and fast gantry rotation (330 msec), potentially permit a noninvasive assessment of coronary anatomy, global and regional LV function, and perfusion defects (PDs) and delayed enhancement. Data on the accuracy of coronary artery assessment is rapidly evolving, with many articles showing high sensitivity and specificity for detection of substantial coronary artery stenosis by using multidetector CT as compared with invasive coronary angiography (3–7). While promising reports on ventricular function (8–12) and infarct imaging by using multidetector CT (13–16) have been published, data on global LV function, regional wall motion (RWM), and PD assessment with multidetector CT in the acute MI setting are somewhat limited. If these assessments can be reliably obtained by using multidetector CT, it may provide an excellent tool for the rapid noninvasive diagnostic and prognostic evaluation of patients with acute MI. We hypothesized that 64-section multidetector CT is able to identify patients with acute MI on the basis of the assessment of global and regional LV function and myocardial perfusion. Thus, the purpose of our study was to assess the accuracy of 64-section multidetector CT for the assessment of PD, RWM, and global LV function.

Portability and Accountability Act compliant. A total of 102 patients who underwent 64-section multidetector CT scanning and transthoracic echocardiography (TTE) were studied in two groups. Group 1 consisted of 34 consecutive patients, who were prospectively enrolled with written informed consent from January to October 2005, and who had suffered a first episode of ST segment elevation MI. Patients with previous MI, coronary bypass grafting, unstable conditions, and frequent arrhythmias were excluded ($n = 22$). Group 1 patients underwent multidetector CT scanning and TTE 3–5 days after percutaneous coronary intervention for reperfusion. TTE and multidetector CT studies were performed on the same day in 28 patients and 1 day apart in the remaining six. Group 2 consisted of 68 consecutive patients with no prior history of acute MI (controls) who underwent TTE and 64-section multidetector CT within a week of each other without a change in clinical status between the two studies. Group 2 patients were retrospectively enrolled with multidetector CT dates between January and October 2005 with waiver of informed consent from our institutional review board. As in group 1, patients with previous MI,

Advances in Knowledge

- Patients with acute myocardial infarction (MI) can be identified by using 64-section multidetector CT on the basis of regional wall motion abnormalities and myocardial perfusion defects with a sensitivity of 94% and a specificity of 97%.
- Global ($r = 0.68$) and regional ($\kappa = 0.79$) left ventricular function had good correlation between 64-section multidetector CT and electrocardiography.
- Multidetector CT helped detect hypoenhanced myocardium in patients after acute MI, and quantification of infarct size by using multidetector CT had a good correlation as compared with cardiac enzymes ($r = 0.82$ for creatinine phosphokinase, $r = 0.76$ for creatinine phosphokinase of the muscle band, and $r = 0.75$ for troponin) and moderate correlation as compared with SPECT ($r = 0.48$, $-7\% \pm 9$).

Materials and Methods

Patient Population

This study was institutional review board approved and Health Insurance

Implications for Patient Care

- Functional and perfusion assessment by using multidetector CT may have a role in the diagnosis, management, and risk stratification of patients with acute MI.
- In addition to coronary imaging, evaluation of function and perfusion by using multidetector CT may help in the detection of patients with acute coronary syndrome.

Published online

10.1148/radiol.2482071478

Radiology 2008; 248:466–475

Abbreviations:

EF = ejection fraction
 LV = left ventricular
 MI = myocardial infarction
 PD = perfusion defect
 RWM = regional wall motion
 TTE = transthoracic echocardiography

Author contributions:

Guarantor of integrity of entire study, R.C.C.; study concepts/study design or data acquisition or data analysis/interpretation, all authors; manuscript drafting or manuscript revision for important intellectual content, all authors; approval of final version of submitted manuscript, all authors; literature research, R.C.C., M.D.S.; clinical studies, all authors; statistical analysis, R.C.C., M.F.; and manuscript editing, all authors

Funding:

This work was supported by the National Institutes of Health (grant 1 T32 HL076136-02).

coronary bypass grafting, unstable conditions, and frequent arrhythmias were excluded ($n = 27$).

In addition, patients with an abnormal ejection fraction (EF) detected at echocardiography were excluded from the control group ($n = 9$). The clinical reasons for multidetector CT in patients without acute MI was to rule out significant coronary artery disease in patients with atypical chest pain ($n = 60$), assessment of coronary artery anomaly ($n = 4$), and evaluation of the thoracic aorta ($n = 4$).

Baseline characteristics of all patients were recorded including patient age, sex, history of diabetes, hypertension, dyslipidemia, smoking history, and family history of premature cardiovascular events. Cardiac biomarkers for myocardial injury were assessed in the acute MI patients.

Multidetector CT Imaging

All multidetector CT examinations were performed with a 64-section scanner (Sensation 64; Siemens Medical Solutions, Forchheim, Germany). In preparation for the scan, all patients with a heart rate above 65 beats/min ($n = 56$, 55%) received a beta-blocker (5 mg of metoprolol intravenously for a maximum of 15 mg) unless their systolic blood pressure was less than 100 mm Hg, and had moderate to severe aortic stenosis, symptomatic asthma or emphysema or had previous known allergies. Imaging parameters were collimation, 32×0.6 mm; gantry rotation, 330 msec; tube voltage, 120 kV; effective tube current-time product, 850 mAs; beam pitch, 0.24; table speed, 9.2 mm per rotation. Eighty to 100 mL of contrast medium (320 g per milliliter of iodixanol; Visipaque, GE Healthcare, Princeton, NJ) was injected intravenously at a rate of 4–5 mL/sec followed by 40 mL of saline at the same rate. The delay between the beginning of contrast material administration and scanning was, on average, 24 seconds (range, 18–32 seconds). Breath hold scan time varied from 11 to 16 seconds.

Overlapping transaxial images were reconstructed by using a medium-sharp convolution kernel (B25f) with a section

thickness of 1.5 mm and an increment of 1.5 mm by using an echocardiographically gated half-scan algorithm if the heart rate is less than 62 beats/min or multisegment reconstruction if the heart rate is more than 62 beats/min, with a resulting temporal resolution varying between 82 and 165 msec in the center of rotation. Image reconstruction was retrospectively gated to the electrocardiogram and 16 phases were reconstructed throughout the cardiac cycle (every 6.25% of the R-R interval).

Measurements of radiation exposure for the electrocardiographically gated multidetector CT scans were obtained using a Monte Carlo-based technique.

Multidetector CT Analysis

Multidetector CT analysis was performed with software (Circulation; Siemens Medical Solutions) by two independent experienced cardiac radiologists (R.C.C. and C.H.N., with 6 and 3 years experience in cardiac imaging, respectively) who were blinded to clinical history, cardiac catheterization, echocardiography, and coronary CT angiography data sets. Cardiac CT data sets were randomly presented to radiologists for interpretation and the radiologists were blinded to all information, including to which group the patient belonged. The observers performed several analyses.

Myocardial perfusion analysis.—Evaluation of myocardial perfusion was performed by using 8-mm thick multiplanar reformation, with short-axis sections reconstructed during mid diastole to minimize motion artifacts. Images were displayed by using a narrow window-level display (width, 150 HU; level, 100 HU). Total size of hypoenhanced myocardium was measured manually by using direct planimetry, and expressed as a percentage of the total LV myocardial mass. Myocardium mass was calculated by using the Simpson method, tracing epicardial and endocardial contours in the stack of short-axis images. Hounsfield unit values for the PD, perinfarct region, and remote myocardium were calculated by placing a 0.1-cm^2 region of interest in the desired area.

Qualitative assessment of RWM.—Qualitative assessment of systolic function and RWM was performed by using interactive evaluation of short-axis sections in cine mode. The myocardium was divided in 17 standardized segments by using the American Heart Association/American College of Cardiology classification (17). A four-point scale was used to grade each myocardial segment as normal (grade 3), hypokinetic (grade 2), akinetic (grade 1), or dyskinetic (grade 0).

Global LV function.—End-diastolic volume, end-systolic volume and EF were measured and calculated by using a threshold level-based LV segmentation method (Circulation; Siemens). This method calculates the end-diastolic volume and end-systolic volume on a per-pixel basis after appropriate definition of the mitral valve plane and the LV cavity, excluding the LV outflow tract (18).

Detection of acute MI.—The presence of acute MI was assessed for each patient on the basis of matching RWM abnormalities and myocardial hypoenhancement (perfusion defect) in the same coronary distribution and without further clinical or angiographic information.

TTE Examinations

TTE examinations were performed by using a standard echocardiograph (Sonos 7500; Philips Medical Systems, Andover, Mass). To evaluate RWM, short-axis sections were recorded at the mitral valve, papillary muscle, and apical levels. Additional apical four- and two-chamber long-axis views were evaluated. Two experienced independent echocardiologists (M.D.S. and D.S.J., with 3 and 4 years experience, respectively) calculated the EF by using the modified Simpson method (19). EF was defined as normal ($\geq 55\%$), mildly reduced (46%–54%), and reduced ($\leq 45\%$) by using TTE examinations. The blinded observers qualitatively graded the systolic function and RWM by using the same criteria as did the multidetector CT (17-segment model by using a four-point scale).

SPECT Scanning

SPECT scanning was performed on 44 patients (20 in group 1 with acute MI and 24 in group 2 without). In group 1, SPECT was performed either on the same day of multidetector CT or with 1 day of difference. In group 2, SPECT was performed within 3 days ± 5 (range, 1–8 days) of multidetector CT.

Two observers (T.Y. and a nonauthor, both with more than 10 years experience with nuclear cardiology) interpreted the SPECT images by consensus. In group 1, patients were injected with 10 mCi (370 MBq) of technetium 99m-sestamibi at rest and ungated SPECT myocardial perfusion images were acquired by using a dual-detector gamma

camera with 64 projections, 25 seconds each, in a circular 180° orbit. In group 2, patients underwent the same resting protocol; additionally, an exercise (n = 15) or pharmacologic stress test (n = 9) (intravenous adenosine infusion [maximum dose = 140 µg/kg/min for 5 minutes]) was performed with another dose of 30 mCi (1110 MBq) of technetium 99m-sestamibi injected intravenously at peak drug effect. After 30–60 minutes, gated SPECT images were obtained and assessed for myocardial perfusion. Infarct size and myocardial mass by using SPECT were determined with automated three-dimensional software (4DM; University of Michigan, Ann Arbor, Mich) (20,21).

Infarct-related Artery

For each patient with ST segment elevation MI, an infarct-related artery was defined on the basis of invasive angiography results. The vessel with the most substantial stenosis or occlusion seen at invasive angiography and with the dis-

Baseline Patient Characteristics

Characteristic	All (n = 102)	Control (n = 68)	Acute MI (n = 34)	P Value
Age (y)	57 ± 16*	55 ± 17*	59 ± 14*	.18
No. of Men	65 (64)	38 (56)	27 (79)	.03
Diabetes	12 (12)	9 (13)	3 (9)	.52
Hypertension	54 (53)	34 (50)	20 (59)	.41
Dyslipidemia	53 (52)	27 (40)	26 (76)	<.001
Current smokers	21 (21)	9 (13)	12 (35)	.009
Family history of premature cardiovascular event	20 (20)	9 (13)	11 (32)	.02

Note.—Numbers in parentheses are percentages.

* Data are the mean ± standard deviation.

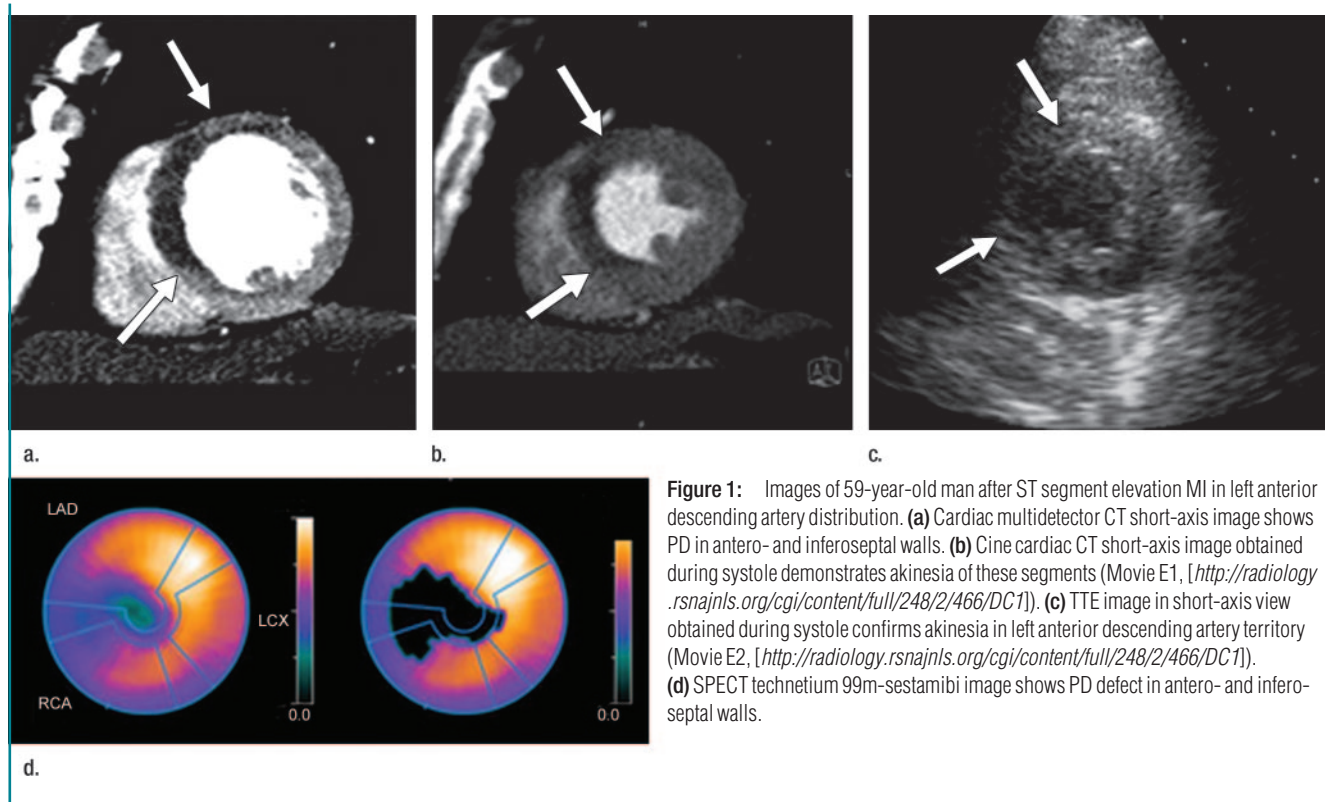
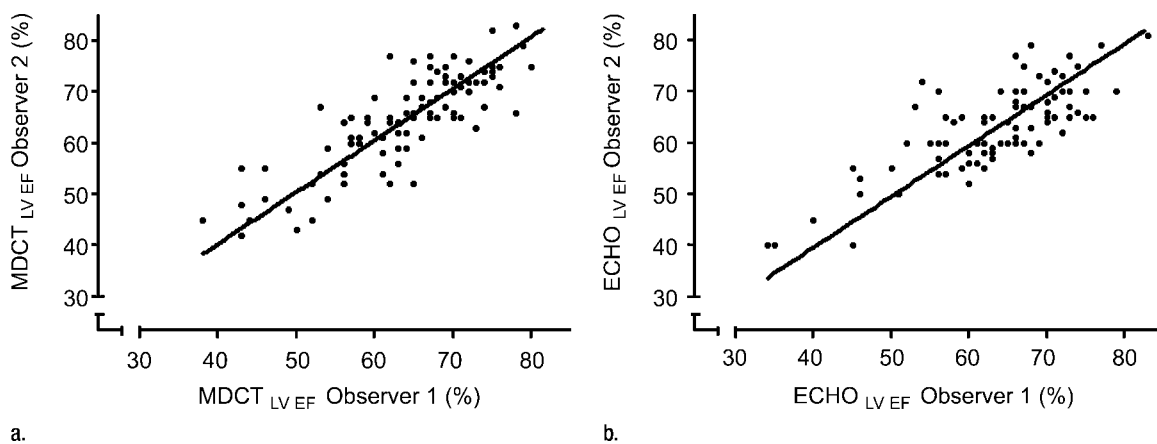
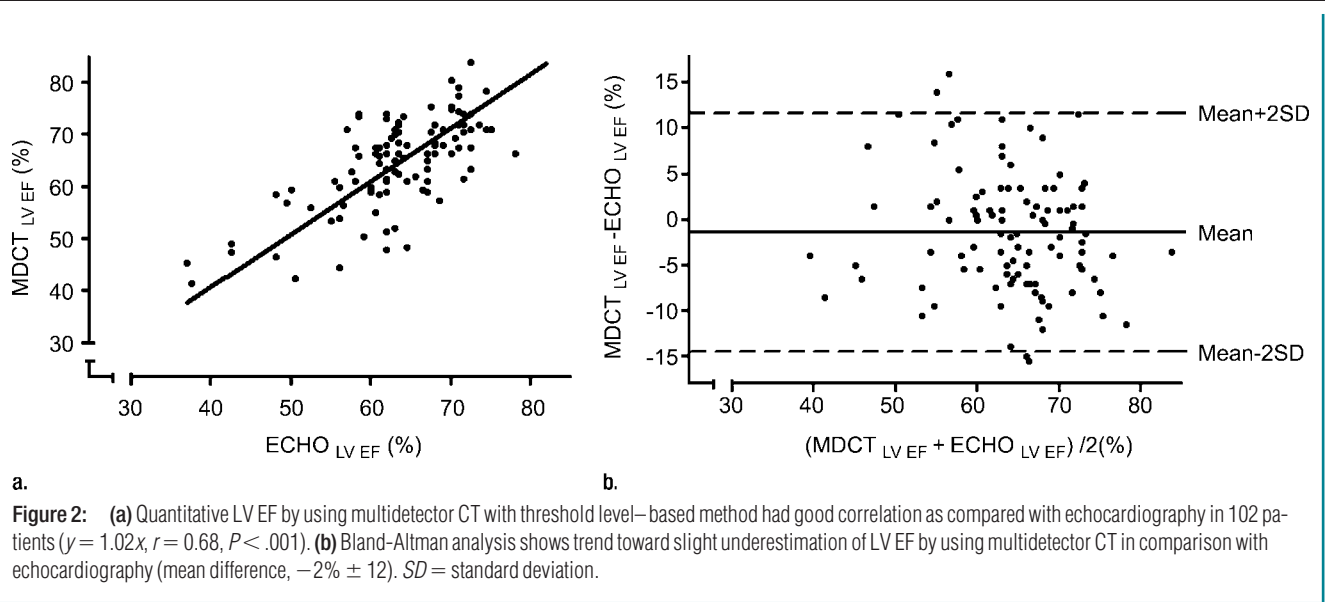


Figure 1: Images of 59-year-old man after ST segment elevation MI in left anterior descending artery distribution. (a) Cardiac multidetector CT short-axis image shows PD in antero- and inferoseptal walls. (b) Cine cardiac CT short-axis image obtained during systole demonstrates akinesia of these segments (Movie E1, [http://radiology.rsnajnl.org/cgi/content/full/248/2/466/DC1]). (c) TTE image in short-axis view obtained during systole confirms akinesia in left anterior descending artery territory (Movie E2, [http://radiology.rsnajnl.org/cgi/content/full/248/2/466/DC1]). (d) SPECT technetium 99m-sestamibi image shows PD defect in antero- and inferoseptal walls.



tribution in agreement with echocardiographic changes was considered the infarct-related artery. Multidetector CT and SPECT were performed within 3–5 days of cardiac catheterization and the invasive angiographic data were correlated to the distribution of the myocardial PD detected by using multidetector CT and SPECT (17).

Comparative Analyses

Descriptive analyses were performed to assess the baseline characteristics

of the patient population. By using the documented clinical diagnosis and invasive angiography results for location of infarct-related artery as the reference, the diagnostic performance of multidetector CT, was determined by using myocardial enhancement and RWM. Interobserver variability was calculated for the investigators assessing EF in multidetector CT and TTE. Similarly, global and regional LV function was compared with TTE. Finally,

PDs were quantitatively assessed and were correlated with peak of cardiac biomarker (creatinine phosphokinase, creatinine phosphokinase of the muscle band fraction, and troponin) levels. For the subset of patients who underwent SPECT myocardial perfusion imaging, the total size of PD as a percentage of the total myocardial mass was compared between multidetector CT and SPECT. Agreement of segmental RWM between multidetec-

tor CT and echocardiography was calculated for the wall motion scores of each of the 17 segments.

Statistical Analysis

All values are expressed as the mean ± standard deviation. The correlation between multidetector CT and TTE for global LV function and between multidetector CT PD and cardiac biomarker levels and SPECT PD was assessed by using a correlation coefficient (*r*) on a per-patient basis. The interobserver variability for the multidetector CT and TTE LV EF assessment and the agreement between multidetector CT and TTE on a per-segment basis for RWM in the overall population and in the acute MI group were assessed by using the κ statistic for categorical variables and the Pearson correlation for continuous variables as follows: poor agreement, κ = 0; slight agreement, κ = 0.01–0.20; fair agreement, κ = 0.21–0.40; moderate agreement, κ = 0.41–0.60; good agreement, κ = 0.61–0.80; and excellent agreement, κ = 0.81–1.00. The

Bland-Altman approach (including the 95% confidence interval) was used to compare the EF measured at multidetector CT and echocardiography and the percentage of PD between multidetector CT and SPECT. The *t* test was used to detect significant differences between ages in the sub-groups. Differences in sex and risk factors were analyzed by using the χ² test. A *P* value of less than .05 was considered to indicate a significant difference. All statistical analyses were performed with software (SPSS, version 14.0; SPSS, Cary, NC).

Results

Patient Population

The mean age of the study population was 57 years ± 16 and 64% of the patients were men (Table 1). On the basis of invasive angiographic results, the left anterior descending, left circumflex, and right coronary arteries were the infarct-related artery in eight, four, and 22 cases of MI, respectively.

Our direct measurements of radiation exposure (22) demonstrated that the mean radiation dose of this cardiac multidetector CT protocol was 13.7 mSv ± 3.4.

Detection of Patients with Acute MI

Cardiac multidetector CT helped demonstrate a matched PD and abnormal RWM in 32 of 34 patients with clinically diagnosed acute MI (Fig 1), and absence of a matched PD and abnormal RWM in 68 patients, two of which had a clinical diagnosis of acute MI. Thus, a sensitivity of 94% (32 of 34), a specificity of 97% (66 of 68), a positive predictive value of 94% (32 of 34), a negative predictive value of 97% (66 of 68), and an overall accuracy of 96% (98 of 102) were obtained to help detect acute MI. The interobserver correlation for the detection of acute MI by using multidetector CT was excellent (κ = 0.84). In four cases there was mismatch between PD and RWM. In three cases, a possible hypoperfusion was detected without associated RWM abnormality, and this was considered to be artifact. In one case, there was a possible RWM abnormality at the basal septum but PD was not seen.

TTE helped detect abnormal RWM in 31 of 34 patients (sensitivity, 91%) with acute MI and correctly excluded abnormal RWM in 67 of 68 patients (specificity, 99%) among those without acute MI. Positive and negative predictive values and accuracy for TTE to help detect acute MI on the basis of RWM were 97%, 96%, and 96%, respectively.

Global LV Function by Using Multidetector CT and TTE

The mean LV EF ± standard deviation measured by using TTE and multidetector CT was 65% ± 9 versus 63% ± 8 for all patients, 60% ± 9 versus 57% ± 10 for acute MI patients, and 67% ± 7 versus 64% ± 9 for nonacute MI patients, respectively. Overall, the respective numbers of patients with normal, mildly reduced, and reduced EF were 87, 10, and five patients by using multidetector CT and 89, eight, and five patients by using TTE. Results for multide

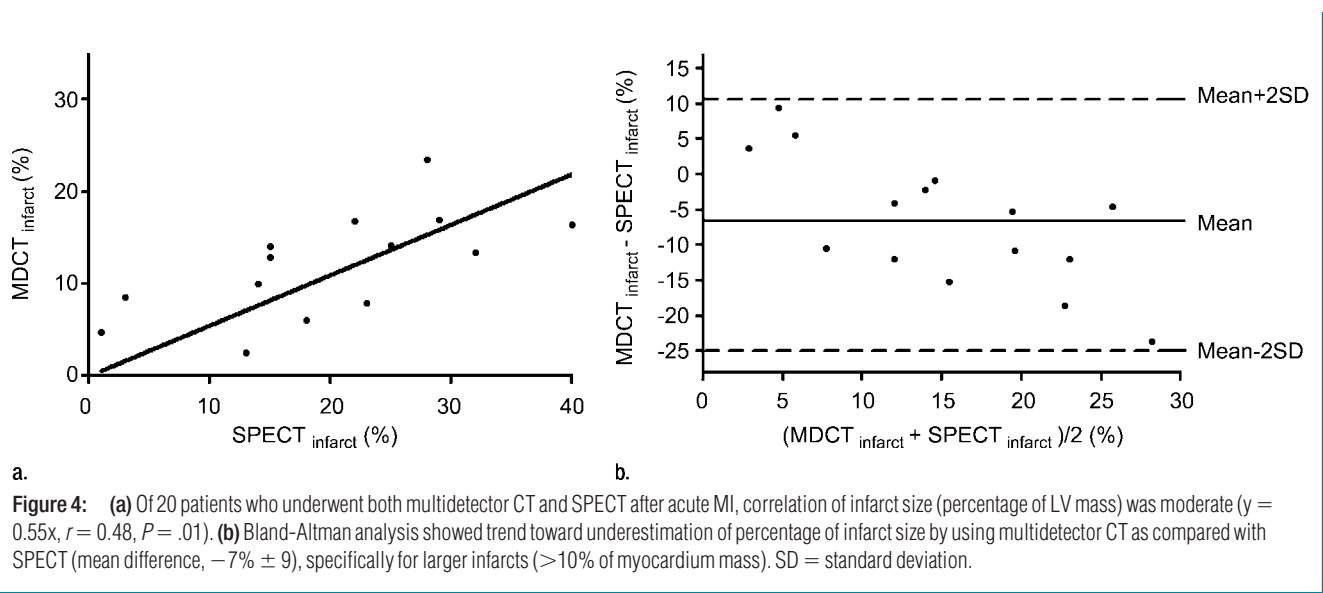
Agreement between Multidetector CT and Echocardiography for RWM Abnormalities in All 102 Patients

Multidetector CT	Echocardiography			Total
	Akinesis	Hypokinesis	Normal	
Akinesis	32	3	2	37
Hypokinesis	13	112	29	154
Normal	4	19	1520	1543
Total	49	134	1551	1734

Agreement between Multidetector CT and Echocardiography for the Acute MI Group

Multidetector CT	Echocardiography			Total
	Akinesis	Hypokinesis	Normal	
Akinesis	32	3	0	35
Hypokinesis	13	110	23	146
Normal	4	15	378	397
Total	49	128	401	578

There were 34 acute MI patients.



tector CT and TTE for EF had a good correlation for the overall group ($r = 0.68$) (Fig 2), patients with acute MI ($r = 0.69$), and patients without acute MI ($r = 0.67$). Bland-Altman analysis revealed a trend of multidetector CT slightly underestimating LV EF compared with TTE (mean difference, $-2\% \pm 12$) (Fig 2). The interobserver reliability for assessment of global LV EF with multidetector CT was excellent ($r = 0.83$). The interobserver reliability for assessment of global LV EF with echocardiography was good ($r = 0.68$) (Fig 3).

Assessment of RWM by Using Multidetector CT and TTE

There was excellent correlation between RWM by using multidetector CT and clinical assessment of acute MI territory ($\kappa = 0.82$). The agreement between multidetector CT and TTE for RWM on a four-point scale on the basis of the 17-segment model was good (1664 of 1734 segments, 96%; $\kappa = 0.79$) (Table 2). When the analysis was performed only in patients with clinical acute MI the agreement remained good (520 of 578 segments, 90%; $\kappa = 0.78$) (Table 3). Finally, the interobserver correlation between two observers for multidetector CT RWM assessment was excellent on a per-patient (0.83) and a per-segment (0.80) basis.

Myocardial PD by Using Multidetector CT and SPECT

Of the 34 patients with PD detected by using multidetector CT, 32 correlated with the correct coronary artery distribution of the culprit lesion, as defined by invasive coronary angiography. The mean Hounsfield units for PD by using multidetector CT was $50 \text{ HU} \pm 12$ (range, 16–75 HU), perinfarct region was $70 \text{ HU} \pm 13$ (range, 40–102 HU), and remote myocardium was $99 \text{ HU} \pm 14$ (range, 77–142 HU). Peak cardiac biomarkers among patients with acute MI were as follows: creatinine phosphokinase, $1963 \text{ U/L} \pm 1763$; creatinine phosphokinase of the muscle band fraction, $222 \text{ U/L} \pm 222$; and troponin, $5.4 \mu\text{g/L} \pm 4.2$. The overall LV mass was $131 \text{ g} \pm 36$ by using multidetector CT versus $141 \text{ g} \pm 23$ by using SPECT ($r = 0.40$). The mean PD percentage was $11\% \pm 5$ by using multidetector CT and $15\% \pm 13$ by using SPECT in patients with acute MI. There was moderate correlation between percentage of infarct size as determined by using multidetector CT versus SPECT in 20 patients who underwent SPECT scanning with acute MI ($r = 0.48$) (Fig 4). Bland-Altman analysis showed a trend toward multidetector CT resulting in underestimation of percentage of infarct size for

larger infarcts and overestimation for smaller infarcts as compared with SPECT (mean difference, $-7\% \pm 9$) (Fig 4). Of 20 patients with acute MI who had infarcts, SPECT helped detect nine inferior MIs, five anterior MIs, and one lateral MI. However, SPECT did not help detect subendocardial infarcts in five patients (four had inferior MIs, one had a lateral MI) who were detected by using multidetector CT and had clinically proved ST segment elevation MI with increased cardiac enzymes and coronary occlusion, as defined by using cardiac catheterization (Fig 5). Cardiac multidetector CT excluded PD in 24 patients without acute MI who underwent SPECT. Finally, there was good to excellent linear correlation among all three cardiac serum biomarkers and the PD percentage by using multidetector CT ($r = 0.82$ for peak creatinine phosphokinase, $r = 0.76$ for creatinine phosphokinase of the muscle band, and $r = 0.75$ for troponin).

Discussion

In our study, 64-section multidetector CT not only demonstrated a good correlation for the assessment of LV EF as compared with TTE, but excellent interobserver variability, as well. Fur-

thermore, detection of abnormal RWM by using a 17-segment model showed good correlation with TTE. Moreover, quantification of PD by using multidetector CT as a percentage of total LV mass had excellent correlation with cardiac biomarkers and moderate correlation with SPECT quantification of infarct size. Finally, the comprehensive multidetector CT analysis for detection of acute MI on the basis of matching PD and abnormal RWM yielded a sensitivity of 94% and specificity of 97%, and showed that the inter-

observer reliability was better with multidetector CT ($r = 0.83$) as compared with TTE ($r = 0.68$).

Global and Regional LV Function

Assessment of global and regional ventricular function with any imaging modality requires high temporal resolution. In our study, assessment of the global LV function by using multidetector CT showed excellent reproducibility and good correlation with TTE, which confirms earlier comparisons of four- and 16-section multidetector CT with TTE and MR (8–12).

Although the temporal resolution of multidetector CT (82–165 msec) is still inferior to that of TTE, we found that abnormal systolic function in terms of RWM could be discerned in almost all cases of MI. Further, multidetector CT was not limited by poor acoustic echocardiographic windows. It is also important to point out that the detection of acute MI in patients by using multidetector CT was not inferior to that of TTE (similar accuracy of 96%) and that the interobserver reliability for EF quantification was better with multidetector CT ($r = 0.83$), as compared with TTE ($r = 0.68$).

Myocardial Perfusion

Detection of PD can be accomplished by using numerous imaging modalities such as SPECT, positron emission tomography, contrast-enhanced echocardiography, and MR imaging. Compared with histopathologic analysis or delayed-enhancement MR imaging, multidetector CT perfusion imaging underestimates infarct size (15,23,24). Nevertheless, it is still regarded as a useful tool for detection of acute permanent PDs and may represent a combination of microvascular obstruction and myocardial necrosis (13,25). In our study, infarct size determined by using multidetector CT had an excellent correlation with cardiac biomarkers and moderate correlation with SPECT but with systematic underestimation as compared with SPECT, specifically for larger infarcts. However, multidetector CT helped detect subendocardial PD in five patients with a clinical diagnosis of acute MI that SPECT did not (proved with coronary occlusion at cardiac catheterization, increased cardiac enzymes, and matched RWM abnormality). One reason that subendocardial infarcts might not be identified by using SPECT is the fairly poor spatial resolution of about $10 \times 10 \times 10$ mm full width at half maximum, as compared with the superior spatial resolution of 64-section multidetector CT ($0.4 \times 0.4 \times 0.6$ mm). Furthermore, the limitations of SPECT in the detection of subendocardial MIs are well recognized, having cardiac MR imaging and histologic analysis as refer-

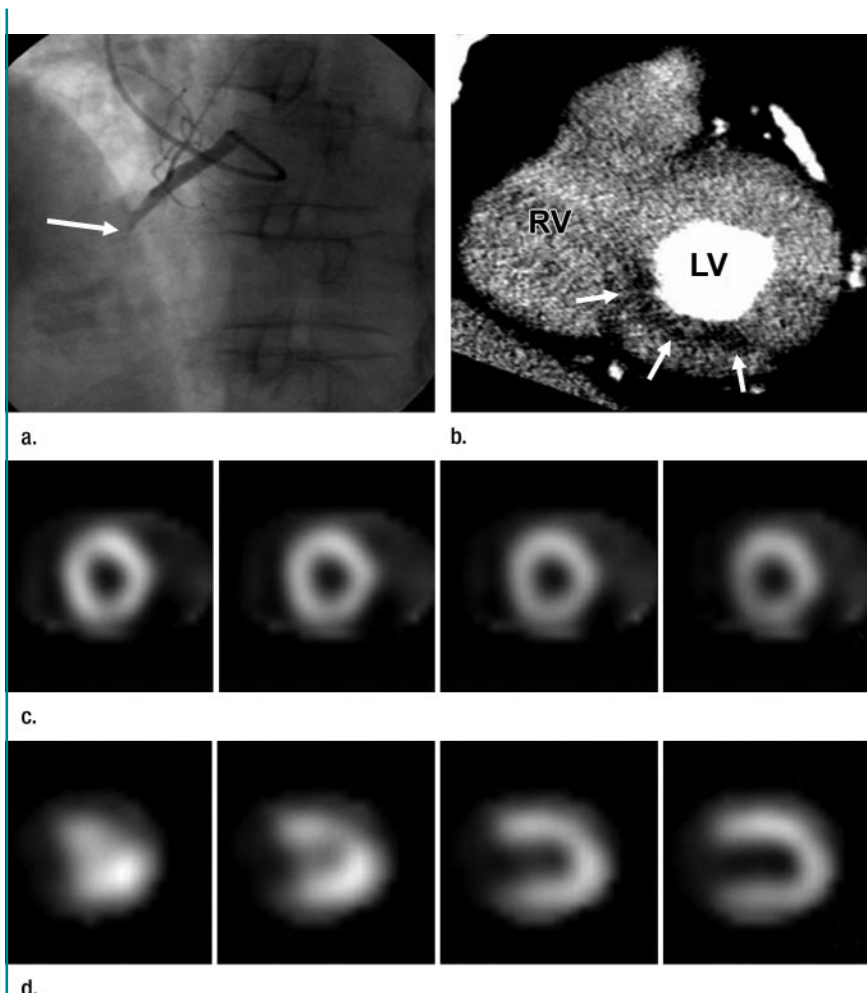


Figure 5: Images of 67-year-old man with substernal chest pain and 4-mm ST segment elevation on echocardiogram. **(a)** Coronary angiogram shows total occlusion of proximal right coronary artery (arrow) that was successfully stented. **(b)** Multidetector CT study 5 days later reveals area of hypoperfusion (arrows) in inferoseptal and inferior walls, representing MI. Patient also underwent SPECT myocardial perfusion imaging at rest for determination of infarct size on same day of CT. **(c)** Short-axis and **(d)** vertical long-axis images did not reveal PD.

ence standards (26). Moreover, we emphasize the clinical importance that even small subendocardial infarcts can influence prognosis and carry a high cardiac risk with incremental prognostic value to major cardiac events and cardiac mortality beyond common clinical, angiographic, and functional predictors (27). A more accurate estimation of infarct size may be accomplished with delayed-enhancement multidetector CT by performing a second scan between 5 and 15 minutes after contrast agent injection (23–25). However, a delayed scan increases total radiation exposure and requires a higher dose of contrast agent to allow differentiation of infarcted and normal myocardium (28).

Our direct measurements of radiation exposure were 13 mSv. To put this in perspective, the radiation doses associated with stress SPECT technetium 99m-sestamibi and stress SPECT thallium examinations are approximately 12 mSv and 25 mSv, respectively (28).

Clinical Implications

In the clinical setting, when a patient presents with acute chest pain and electrocardiographic changes, the diagnosis of acute MI is usually obvious and cardiac catheterization is the next step. However, multidetector CT may be used in patients where the diagnosis of acute coronary syndrome is unclear, such as in patients presenting with acute chest pain to the emergency department with nondiagnostic electrocardiogram and negative initial levels of cardiac enzymes. The assessment of infarct size, the detection of dysfunctional but viable tissue, and the evaluation of global and regional function have prognostic value. Multidetector CT may provide an alternative means to existing imaging modalities for risk stratification and management after acute MI. It remains to be seen if this information may improve diagnostic accuracy of coronary multidetector CT angiography in helping detect patients with significant stenosis or acute coronary syndromes. Multidetector CT myocardial perfusion evaluation may even allow distinction of acute and chronic MI (29) or help predict myocardial viability and LV func-

tional recovery (30). These functional data are readily available for every cardiac multidetector CT examination without the need for further scanning, contrast administration, or exposure to extra radiation.

Our study had several limitations. Multidetector CT scans in acute MI patients were obtained after treatment of ST segment elevation MI. This precluded the multidetector CT assessment of culprit lesions. Myocardial PD, as assessed by using multidetector CT, identifies infarction but underestimates total infarct size, specifically for larger infarcts. Delayed enhancement multidetector CT imaging, similar to delayed enhancement MR imaging, has been reported recently and may provide more accurate estimation of infarct size, at the expense of more contrast and radiation exposure. There was some disagreement between TTE and multidetector CT for RWM abnormality assessment. The main reason for this discrepancy likely resulted from lack of perfect coregistration and subjective analysis performed by using both multidetector CT and TTE. Another limitation for cardiac multidetector CT is that patients with atrial fibrillation or heart rate abnormalities may result in impaired image quality and may limit the application of this technique in this population.

In conclusion, 64-section multidetector CT can accurately assess global and regional LV function and resting myocardial PDs in patients with and without acute MI. Comprehensive assessment of these functional parameters by using multidetector CT allows accurate detection of acute MI and may have prognostic implications.

References

- Jacobs AK, Antman EM, Ellrodt G, et al. Recommendation to develop strategies to increase the number of ST-segment-elevation myocardial infarction patients with timely access to primary percutaneous coronary intervention. *Circulation* 2006;113(17):2152–2163.
- Antman EM, Anbe DT, Armstrong PW, et al. ACC/AHA guidelines for the management of patients with ST-elevation myocardial infarction: executive summary—a report of the ACC/AHA Task Force on Practice

Guidelines. *Circulation* 2004;110(5):588–636.

- Leschka S, Alkadhi H, Plass A, et al. Accuracy of MSCT coronary angiography with 64-slice technology: first experience. *Eur Heart J* 2005; 26:1482–1487.
- Leber AW, Knez A, von Ziegler F, et al. Quantification of obstructive and nonobstructive coronary lesions by 64-slice computed tomography: a comparative study with quantitative coronary angiography and intravascular ultrasound. *J Am Coll Cardiol* 2005; 46:147–154.
- Raff GL, Gallagher MJ, O'Neill WW, Goldstein JA. Diagnostic accuracy of non-invasive coronary angiography using 64-slice spiral computed tomography. *J Am Coll Cardiol* 2005;46:552–557.
- Mollet NR, Cademartiri F, van Mieghem CA, et al. High-resolution spiral computed tomography coronary angiography in patients referred for diagnostic conventional coronary angiography. *Circulation* 2005;112:2318–2323.
- Ropers D, Rixe J, Anders K, et al. Usefulness of multidetector row spiral computed tomography with 64 × 0.6-mm collimation and 330-ms rotation for the noninvasive detection of significant coronary artery stenoses. *Am J Cardiol* 2006;97:343–348.
- Juergens KU, Grude M, Maintz D, et al. Multi-detector row CT of left ventricular function with dedicated analysis software versus MR imaging: initial experience. *Radiology* 2004;230:403–410.
- Mahnken AH, Koos R, Katoh M, et al. Sixteen-slice spiral CT versus MR imaging for the assessment of left ventricular function in acute myocardial infarction. *Eur Radiol* 2005;15(4):714–720.
- Schlosser T, Pagonidis K, Herborn CU, et al. Assessment of left ventricular parameters using 16-MDCT and new software for endocardial and epicardial border delineation. *AJR Am J Roentgenol* 2005;184:765–773.
- Raman SV, Shah M, McCarthy B, Garcia A, Ferketich AK. Multi-detector row cardiac computed tomography accurately quantifies right and left ventricular size and function compared with cardiac magnetic resonance. *Am Heart J* 2006;151:736–744.
- Sugeng L, Mor-Avi V, Weinert L, et al. Quantitative assessment of left ventricular size and function: side-by-side comparison of real-time three-dimensional echocardiography and computed tomography with magnetic resonance reference. *Circulation* 2006; 114:654–661.
- Hoffmann U, Millea R, Enzweiler C, et al. Acute myocardial infarction: contrast-en-

- hanced multi-detector row CT in a porcine model. *Radiology* 2004;231(3):697-701.
14. Wada H, Kobayashi Y, Yasu T, et al. Multi-detector computed tomography for imaging of subendocardial infarction: prediction of wall motion recovery after reperfused anterior myocardial infarction. *Circ J* 2004;68(5):512-514.
 15. Nikolaou K, Sanz J, Poon M, et al. Assessment of myocardial perfusion and viability from routine contrast-enhanced 16-detector-row computed tomography of the heart: preliminary results. *Eur Radiol* 2005;15(5):864-871.
 16. Mahnken AH, Bruners P, Katoh M, Wildberger JE, Gunther RW, Buecker A. Dynamic multi-section CT imaging in acute myocardial infarction: preliminary animal experience. *Eur Radiol* 2006;16(3):746-752.
 17. Cerqueira MD, Weissman NJ, Dilsizian V, et al. Standardized myocardial segmentation and nomenclature for tomographic imaging of the heart. *Circulation* 2002;105:539-542.
 18. Juergens KU, Fischbach R. Left ventricular function studied with MDCT. *Eur Radiol* 2006;16(2):342-357.
 19. Schiller NB, Acquatella H, Ports TA, et al. Left ventricular volume from paired biplane two-dimensional echocardiography. *Circulation* 1979;60(3):547-555.
 20. Kang X, Berman DS, Van Train KF, et al. Clinical validation of automatic quantitative defect size in rest technetium-99 m-sestamibi myocardial perfusion SPECT. *J Nucl Med* 1997;38:1441-1446.
 21. Germano G, Kavanagh PB, Waechter P, et al. A new algorithm for the quantitation of myocardial perfusion SPECT. I. Technical principles and reproducibility. *J Nucl Med* 2000;41:712-719.
 22. Jones DG, Shrimpton PC. Normalised organ doses for X-ray computed tomography calculated using Monte Carlo techniques. NPRB-SR250. Chilton, England: National Radiological Protection Board, 1993.
 23. Gerber BL, Belge B, Legros GJ, et al. Characterization of acute and chronic myocardial infarcts by multidetector computed tomography: comparison with contrast-enhanced magnetic resonance. *Circulation* 2006;113(6):823-833.
 24. Mahnken AH, Koos R, Katoh M, et al. Assessment of myocardial viability in reperfused acute myocardial infarction using 16-slice computed tomography in comparison to magnetic resonance imaging. *J Am Coll Cardiol* 2005;45(12):2042-2047.
 25. Lardo AC, Cordeiro MA, Silva C, et al. Contrast-enhanced multidetector computed tomography viability imaging after myocardial infarction: characterization of myocyte death, microvascular obstruction, and chronic scar. *Circulation* 2006;113:394-404.
 26. Wagner A, Mahrholdt H, Holly TA, et al. Contrast-enhanced MRI and routine single photon emission computed tomography (SPECT) perfusion imaging for detection of subendocardial myocardial infarcts: an imaging study. *Lancet* 2003;361:374-379.
 27. Kwong RY, Chan AK, Brown KA, et al. Impact of unrecognized myocardial scar detected by cardiac magnetic resonance imaging on event-free survival in patients presenting with signs or symptoms of coronary artery disease. *Circulation* 2006;113(23):2733-2743.
 28. Perisinakis K, Theocharopoulos N, Karkavitsas N, Damilakis J. Patient effective radiation dose and associated risk from transmission scans using Gd-153 line sources in cardiac SPECT studies. *Health Phys* 2002;83:66-74.
 29. Nieman K, Cury RC, Ferencik M, et al. Differentiation of recent and chronic myocardial infarction by cardiac computed tomography. *Am J Cardiol* 2006;98(3):303-308.
 30. Lessick J, Dragu R, Mutlak D, et al. Is functional improvement after myocardial infarction predicted with myocardial enhancement patterns at multidetector CT? *Radiology* 2007;244(3):736-744.